JACS
JOURNAL OF THE AMERICAN CHEMICAL SOCIETY

COMMUNICATION

pubs.acs.org/JACS

Li Ion Diffusion in the Anode Material $Li_{12}Si_7$: Ultrafast Quasi-1D Diffusion and Two Distinct Fast 3D Jump Processes Separately Revealed by ^{7}Li NMR Relaxometry

Alexander Kuhn,*[,†] Puravankara Sreeraj,[‡] Rainer Pöttgen,[‡] Hans-Dieter Wiemhöfer,[‡] Martin Wilkening,[†] and Paul Heitjans*[,†]

[†]Institute of Physical Chemistry and Electrochemistry, and ZFM - Center for Solid State Chemistry and New Materials, Leibniz University Hannover, Callinstr. 3-3a, 30167 Hannover, Germany

[‡]Institute of Inorganic and Analytical Chemistry, University of Münster, Corrensstr. 28-30, 48149 Münster, Germany

Supporting Information

ABSTRACT: The intermetallic compounds Li_xSi_y have attracted considerable interest because of their potential use as anode materials in Li ion batteries. In addition, the crystalline phases in the Li−Si phase diagram turn out to be outstanding model systems for the measurement of fast Li ion diffusion in solids with complex structures. In the present work, the Li self-diffusivity in crystalline $Li_{12}Si_7$ was thoroughly probed by ^{7}Li NMR spin−lattice relaxation (SLR) measurements. Variable-temperature and -frequency NMR measurements performed in both the laboratory and rotating frames of reference revealed three distinct diffusion processes in $Li_{12}Si_7$. The diffusion process characterized by the highest Li diffusivity seems to be confined to one dimension. It is one of the fastest motions of Li ions in a solid at low temperatures reported to date. The Li jump rates of this hopping process followed Arrhenius behavior; the jump rate was $\sim 10^5$ s^{-1} at 150 K and reached 10^9 s^{-1} at 425 K, indicating an activation energy as low as 0.18 eV.

Silicon is intended to be used as negative electrode material for Li ion batteries. This is mainly due to its extraordinarily high specific capacity, which is a factor of 10 higher than that of conventionally used carbon anodes. Technological problems due to the high volumetric change of Si-based anodes and the resulting loss of capacity during cycling are likely to be overcome.[1−4] In general, high Li diffusivity in electrode materials is greatly favorable for the development of rechargeable batteries with optimum performance. However, in spite of the technological significance of Si-based anodes within the scope of energy storage, data on the diffusion of Li in Li_xSi_y are still rare.[5−7] In particular, there have been no studies of the jump processes by microscopic (i.e., atomic-scale) methods such as NMR spectroscopy.[8,9] The available solid-state NMR techniques are capable of reliably probing Li diffusion parameters over a wide dynamic range.[8−11] In addition to the aforementioned technological relevance in battery research, lithium silicides provide interesting model systems for fundamental ^{7}Li NMR diffusion studies. The phase diagram of lithium and silicon shows five crystalline intermetallic Zintl-like phases: $Li_{21}Si_5$, $Li_{13}Si_4$, Li_7Si_3, $Li_{12}Si_7$, and LiSi.[2,12,13] A metastable crystalline phase with the composition $Li_{15}Si_4$ and amorphous Li_xSi_y also exist. The latter phases are obtained by electrochemical lithiation.[14,15]

Here we report on the Li self-diffusivity in crystalline $Li_{12}Si_7$, which among the lithium silicides shows the most interesting crystallographic structure, containing a one-dimensional (1D) silicon backbone, in particular, which is filled with and surrounded by lithium ions on 13 different crystallographic sites.[16−18] $Li_{12}Si_7$ was prepared from a melt of the elemental starting materials in a niobium tube under dry argon (see below). As confirmed by powder X-ray diffraction (XRD), a pure, crystalline product of orthorhombic $Li_{12}Si_7$ (space group *Pnma*) was obtained.

^{7}Li NMR spectroscopy performed under static conditions (i.e., on nonrotating samples) was used to probe microscopic Li diffusion parameters in the mixed conductor $Li_{12}Si_7$. ^{7}Li NMR line shape measurements are highly useful for classifying materials as ionic conductors in a qualitative manner.[19−21] Quantitative information on the diffusive jump process can be obtained in a rather direct way via variable-temperature ^{7}Li NMR spin−lattice relaxation (SLR) measurements. From diffusion-induced NMR SLR rates, dynamic parameters (i.e., absolute jump rates and activation enthalpies) can be deduced.[19] Moreover, frequency-dependent NMR SLR rate measurements, even when performed on a powder sample, contain valuable information on the dimensionality of the jump process under investigation.[22]

^{7}Li NMR spectra (Figure 1) were recorded over the temperature range from 125 to 723 K at a resonance frequency ($\omega_0/2\pi$) of 155.4 MHz. At 125 K, the line is broad and has a complex shape due to (i) nonaveraged dipole−dipole interactions of the ^{7}Li nuclei, (ii) chemical shift anisotropies, and (iii) interactions of the quadrupole moment of ^{7}Li with the electric field gradients at the various crystallographic Li sites in $Li_{12}Si_7$. At low temperatures T, the line width $\Delta\omega/2\pi$ of the central transition is given by the so-called rigid lattice value $\Delta\omega_{rl}/2\pi$, which is ~16 kHz in the present case. With increasing temperature, dipole−dipole interactions are progressively averaged as a result of the thermally activated motion of the ^{7}Li ions. Significant line narrowing sets in when the Li jump rate (τ^{-1}) becomes comparable to the spectral width $\Delta\omega_{rl}/2\pi$. In the case of $Li_{12}Si_7$, the onset of this motional narrowing was observed at a very low temperature of ~130 K (see Figure 1B). From the inflection point of the corresponding

Received: March 4, 2011
Published: May 30, 2011

dx.doi.org/10.1021/ja2020108 | *J. Am. Chem. Soc.* 2011, 133, 11018–11021

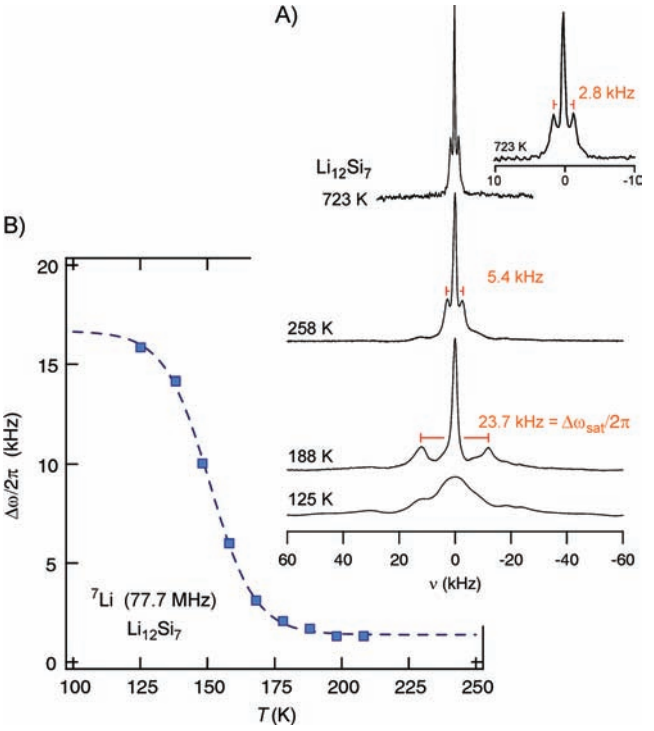

Figure 1. (A) ^{7}Li NMR spectra recorded at various temperatures (125, 188, and 258 K at $\omega_0/2\pi$ = 155.4 MHz and 723 K at 77.7 MHz). The spectral distances of the quadrupolar satellites ($\Delta\omega_{sat}/2\pi$) are indicated. (B) Motional narrowing of the line width (full width at half-maximum) of the central ^{7}Li NMR transition.

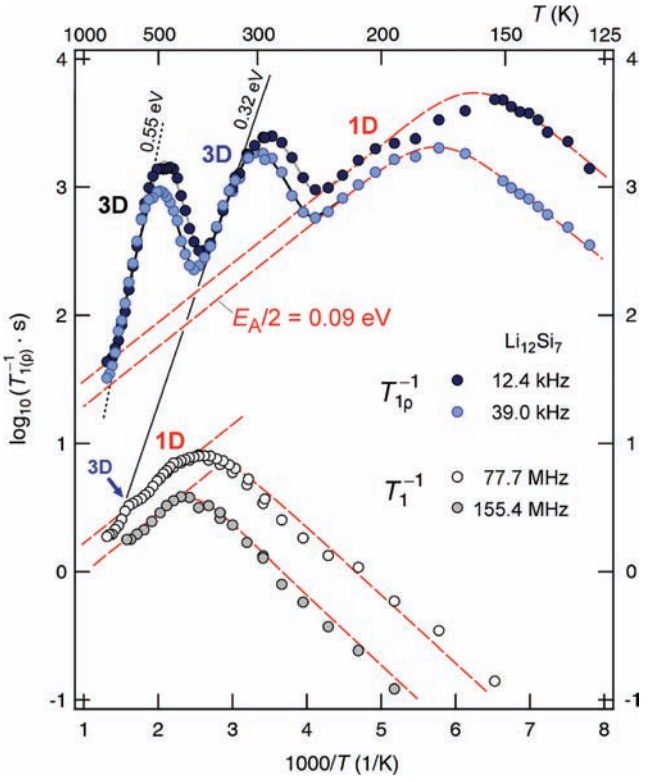

Figure 2. Arrhenius plots of the ^{7}Li NMR SLR rates in the laboratory frame, T_1^{-1}, at $\omega_0/2\pi$ = 155.4 and 77.7 MHz and those in the rotating frame, $T_{1\rho}^{-1}$, at $\omega_1/2\pi$ = 39.0 and 12.4 kHz. Dashed lines are guides to the eye. See the text for further explanation.

narrowing curve $\Delta\omega(T)$ [obtained by plotting $\Delta\omega$ for the central transition (see below) as a function of T], it is possible to obtain a rough estimate of the Li jump rate at the respective temperature via the relation $\tau^{-1} \approx \Delta\omega_{rl}$. It turned out that the rate τ^{-1} was on the order of 10^5 s^{-1} at 150 K.

The ^{7}Li NMR spectra at 188, 258, and 723 K showed the typical shape of the powder spectrum for a spin $^3/_2$ nucleus, consisting of a central transition line and quadrupolar satellite intensities. As can be clearly seen in Figure 1 A, the quadrupolar powder pattern (and thus the mean field gradient experienced by the Li ions) changed with increasing temperature. If it is assumed that the asymmetry parameter of the quadrupolar coupling tensor vanishes, the mean quadrupolar coupling constants δ_Q can be determined from the corresponding spectral distances $\Delta\omega_{sat}/2\pi$ (marked in Figure 1 A by vertical lines pointing to the singularities of the powder pattern) as $\delta_Q = 2 \times \Delta\omega_{sat}/2\pi$. In the present case, δ_Q did not exhibit a gradual change with increasing temperature, as might be ascribed to thermal expansion of the material. Here, as T increased, the satellite intensities gradually vanished, and new ones emerged at even higher temperatures. This behavior can be explained by a stepwise averaging of electric quadrupolar interactions due to Li jump processes between the distinct crystallographic sites in $Li_{12}Si_7$. Thus, at least three different jump processes, each one leading to a specific mean coupling constant δ_Q, were subsequently activated in the silicide, resulting in an intermittent reduction of the electric quadrupole interaction. The mean coupling constants δ_Q were found to be 47.4, 10.8, and 5.6 kHz at 188, 258, and 723 K, respectively.

NMR SLR measurements gave even clearer insight into the lithium dynamics of crystalline $Li_{12}Si_7$. In the Arrhenius plots shown in Figure 2, ^{7}Li NMR SLR rates in the laboratory and rotating frames of reference (T_1^{-1} and $T_{1\rho}^{-1}$, respectively) are shown. The rates were recorded at different resonance ($\omega_0/2\pi$ = 77.7 and 155.4 MHz) and locking ($\omega_1/2\pi$ = 12.4 and 39.0 kHz) frequencies, respectively. Here the NMR SLR is induced solely by local fluctuations of magnetic dipolar or electric quadrupolar interactions due to the motion of the Li spins. As is well-known,[21] these temporal fluctuations can be described in terms of a correlation function $G(\tau')$, and the NMR SLR rate is proportional to the Fourier transform of $G(\tau')$ [i.e., the spectral density $J(\omega_{0(1)})$] at or close to the respective NMR frequency. When purely induced by diffusion processes, the NMR SLR rate passes through a maximum at a characteristic temperature T_{max} at which $1/\tau'$, the correlation rate of the jump process (which is essentially the average jump rate τ^{-1}), equals the NMR frequency (i.e., $\omega \approx \tau^{-1}$). If the NMR SLR rates are measured as a function of T at different resonance frequencies, an absolute jump rate $\tau^{-1}(T_{max})$ can be deduced from each recorded rate peak $T_{1(\rho)}^{-1}(1/T)$. With the use of NMR SLR in the laboratory and rotating frames of reference, both the megahertz and kilohertz ranges can be covered, allowing the determination of the activation energies E_A and the lithium jump rates. The value of $\tau^{-1}(1/T)$ is expected to follow Arrhenius behavior according to the equation $\tau^{-1} = \tau_0^{-1} \exp(-E_A/k_BT)$, where τ_0^{-1} is the pre-exponential factor and k_B is Boltzmann's constant.

Obviously, the global maxima of the two $T_1^{-1}(1/T)$ curves and the low-temperature maxima of the two $T_{1\rho}^{-1}(1/T)$ curves in Figure 2 belong to the same ultrafast diffusion process. The corresponding flanks of the four SLR rate peaks show the same

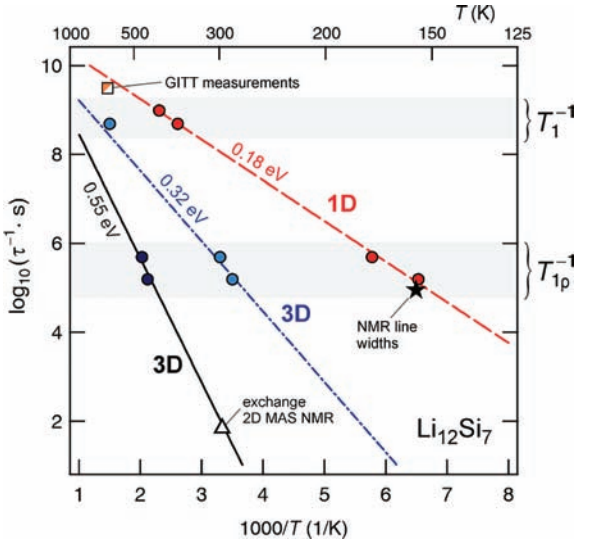

Figure 3. Li jump rates τ^{-1} extracted from the NMR SLR rate maxima of Figure 2; these jump rates are represented by circles. For comparison, the square shows a jump rate derived from literature data (GITT measurements[5]), the star a Li jump rate estimated from the ^{7}Li NMR line narrowing (see Figure 1), and the triangle a Li jump rate from a first 2D exchange MAS NMR measurement.

Table 1. High-Temperature (HT) and Low-Temperature (LT) Limits of the Spectral Density Function $J(\omega)$ for 1D, 2D, and 3D Diffusion[a]

	HT limit	LT limit
1D	$(\tau/\omega)^{0.5}$	$\tau^{-1}\omega^{-\beta}$
2D	$\tau \ln(1/\omega\tau)$	$\tau^{-1}\omega^{-\beta}$
3D	τ	$\tau^{-1}\omega^{-\beta}$

[a] The model parameter β ranges between 1 and 2 and accounts for correlation effects due to Coulomb interactions of the jumping ion or to structural disorder (see ref 8).

slope. The jump rates associated with the peak maxima can be obtained using the maximum conditions $\omega_0 \approx \tau^{-1}$ and $2\omega_1 \approx \tau^{-1}$ (see above).[19,22,23] The resulting rates $\tau^{-1}(T = T_{max})$ are shown in Figure 3 in an Arrhenius plot (red data points). The dashed line represents an Arrhenius fit to the four points, yielding E_A = 0.18 eV. The value of τ_0^{-1} turned out to be on the order of 10^{11} s^{-1}. For comparison, a Li jump rate deduced using galvanostatic intermittent titration technique (GITT) measurements (see ref 5) is also included.

The behavior of the NMR SLR rate flanks [i.e., for temperatures above that of the rate maximum ($\tau^{-1} \gg \omega$) or below it ($\tau^{-1} \ll \omega$)] requires a model-dependent examination. The high-temperature (HT) and low-temperature (LT) limits of $J(\omega)$ according to models for 1D,[22] 2D,[22,24] and 3D[19,22] diffusion in solids are listed in Table 1 (see ref 8). In the case of 3D diffusion, the NMR SLR rate in the high-temperature limit ($\tau^{-1} \gg \omega$) is proportional to τ. As a result, the activation energy derived from that flank should be equal to that obtained from the jump rates $\tau^{-1}(T_{max})$ obtained from the maxima of the SLR rate peaks. Furthermore, the NMR SLR rate on the HT flank is expected to be independent of the resonance frequency applied.[19,22] However, in the present case, *neither* of these predictions was met for the four diffusion-induced SLR rate peaks mentioned above and highlighted in Figure 2 by dashed lines. Interestingly, the NMR SLR rates in the HT limit ($\tau^{-1} \gg \omega$) revealed a distinct frequency dependence. The corresponding HT flanks of the four rate peaks in Figure 2 seem to be parallel (cf. the dashed lines). The apparent activation energy deduced from the HT flanks was approximately half the actual activation energy that was obtained from the jump rates derived from the rate maxima (see the dashed line in Figure 3). These findings are clear indications that the ultrafast diffusion process observed for $Li_{12}Si_7$ is of a low-dimensional nature. According to the theoretical description for 1D diffusion given by Sholl,[22] the diffusion-induced NMR SLR rate on the HT flank is proportional to $\tau^{0.5}\omega^{-0.5}$. Hereby, the factor $\tau^{0.5}$ is responsible for the smaller slope on the HT flank, which is expected to be half the slope in the Arrhenius plot. The factor $\omega^{-0.5}$ brings about the frequency dependence. Although there are many systems in which (quasi) 1D diffusion occurs, in none of these, except for the related phenomenon of 1D diffusion of electron spins,[25] could the theory be checked until now. Essentially, the lack of suitable data stemmed either from the circumstance that the HT flank was not accessible because the diffusion process was too slow or the fact that the HT flank was masked by strong interactions of Li^+ with paramagnetic ions dominating the NMR SLR rate. In the latter case, the NMR SLR rate would no longer be governed solely by Li diffusion. However, in the case of $Li_{12}Si_7$, the two predictions for 1D diffusion were met with satisfying agreement. The apparent activation energy (0.09 eV; see Figure 2) was approximately half the actual one, and the frequency dependence of the SLR rate on the HT flank turned out to be $\sim\omega^{-0.4}$, whereby a frequency range of more than 3 orders of magnitude was covered. Therefore, we assume that this diffusion process is a *quasi*-1D one. Preliminary considerations with regard to the crystal structure and electronic bonding properties of $Li_{12}Si_7$ (see refs 13, 18, and 33) make our assumptions plausible. In particular, the extended structural analysis by Nesper et al.[18] clearly showed the existence of two well-separated 1D infinitesimal partial structure elements along the [100] direction, corresponding to the compositions $[Li_{12}Si_4]$ and $[Li_6Si_5]$. These findings support our conclusion about the quasi-1D or at least strongly anisotropic diffusion process. For comparison, the experimental verification of the predicted spectral density function for Li_xTiS_2 showing pure *2D* diffusion was previously reported by our group.[26]

Apart from this low-dimensional and very fast dynamic process in $Li_{12}Si_7$, the $T_{1\rho}^{-1}(1/T)$ data revealed two additional jump processes showing up as two well-separated ^{7}Li NMR SLR rate peaks at higher temperatures (see Figure 2). The jump rates derived from the corresponding rate maxima are also included in Figure 3 (see the solid and dashed-dotted lines).

The underlying motional processes of the two $T_{1\rho}^{-1}(1/T)$ rate peaks exhibit the characteristics of 3D diffusion, since in both cases the rates on the HT flanks coincide (i.e., the diffusion-induced SLR rates are independent of the locking frequency used). The faster of the two processes caused the $T_{1\rho}^{-1}$ rate to pass through characteristic peak maxima near room temperature (at 3.5 K^{-1} on the 1000/T scale; see Figure 2). Presumably, the same process led to the slight shoulder appearing at $1000/T \approx$ 1.5 K^{-1} on the HT flank of the rate peak $T_1^{-1}(1/T)$ measured at 77.7 MHz (see the arrow in Figure 2). For measurements at 155.4 MHz, only temperatures up to 633 K were accessible with our equipment. This was not high enough to clearly reach the corresponding rate maximum at the largest resonance frequency used. Still, the respective incipient rate peak seems to

be indicated in the SLR rates measured at the highest temperatures and 155.4 MHz. The activation energy of the faster 3D jump process obtained from the three rate maxima (dashed-dotted line in Figure 3) and the one taken from the slope of the HT flank of the rotating-frame SLR rates (solid line in Figure 2) are identical within experimental error (0.32 eV). Beyond doubt, this is expected for a 3D diffusion process (see above and Table 1).

The second 3D process, which is characterized by the highest activation energy, was visible only in the $T_{1\rho}^{-1}(1/T)$ data (see Figure 2). The corresponding Arrhenius line in Figure 3 (black line) is not a fit through the two points obtained from the SLR rate maxima. Here, the activation energy was taken from the HT flank of the rotating-frame SLR rates, yielding E_A = 0.55 eV for this 3D process. The Arrhenius line for this jump process is in very good agreement with the Li jump rate deduced from a first measurement by 2D exchange magic-angle-spinning (MAS) NMR spectroscopy.[27]

As also found for the quasi-1D process, the pre-exponential factors τ_0^{-1}, which are interpreted as attempt frequencies of the two 3D processes, were on the order of 10^{11} s^{-1}. This value is ~2 orders of magnitude lower than the optical phonon Li modes of $Li_{12}Si_7$ obtained from ab initio calculations.[13] Generally, the tendency to have lower pre-exponential factors in the Arrhenius relation in comparison with the phonon frequencies can be understood in terms of cooperative motions or strong anharmonicities of the potential landscape next to a vacancy; the latter might lead to lower vibrational frequencies than in the vacancy-free bulk (for a discussion of low pre-exponential factors obtained by NMR spectroscopy, see, e.g., refs 24, 28, and 29).

In summary, the low-dimensional hopping process found for polycrystalline $Li_{12}Si_7$ (E_A = 0.18 eV) is one of the fastest Li diffusion processes in solids known in the literature. Its quasi-1D nature has been revealed by frequency-dependent NMR SLR measurements. The fast 3D Li jump process (E_A = 0.32 eV), although much slower than the quasi-1D process, is nonetheless comparable to diffusion processes in typical superionic Li conductors.[30−32] The slower 3D process has an activation energy of 0.55 eV, which is similar to that for self-diffusion in lithium metal.[33] To our knowledge, this is the first system in which three distinct Li jump processes, which are activated one after the other according to their increasing jump barriers, have been separately characterized using diffusion-induced NMR SLR measurements.

Subsequent studies will include the identification of the diffusion pathways and sites related to the revealed jump processes. From the structure, even many more than those three distinct jump processes are expected. Presumably, exchange processes between comparable crystallographic sites show similar jump barriers and therefore are not separately seen in NMR relaxometry. 1D and 2D MAS NMR measurements carried out at very low temperatures might help identify the crystallographic sites connected to the three main diffusion processes probed by NMR SLR.

■ ASSOCIATED CONTENT

Supporting Information. Sample preparation and experimental details. This material is available free of charge via the Internet at http://pubs.acs.org.

■ AUTHOR INFORMATION

Corresponding Author
kuhn@pci.uni-hannover.de; heitjans@pci.uni-hannover.de

■ ACKNOWLEDGMENT

Financial support by the BMBF within Project HE-Lion as well as by the DFG (FOR 1277) is greatly appreciated. A.K. gratefully acknowledges financial support by the Studienstiftung des Deutschen Volkes e.V.

■ REFERENCES

(1) Weydanz, W. J.; Wohlfahrt-Mehrens, M.; Huggins, R. A. *J. Power Sources* **1999**, *81*, 237.
(2) Key, B.; Bhattacharyya, R.; Morcrette, M.; Seznéc, V.; Tarascon, J.-M.; Grey, C. P. *J. Am. Chem. Soc.* **2009**, *131*, 9239.
(3) Chan, C. K.; Peng, H.; Liu, G.; McIlwrath, K.; Zhang, X. F.; Huggins, R. A.; Cui, Y. *Nat. Nanotechnol.* **2008**, *3*, 31.
(4) Hertzberg, B.; Alexeev, A.; Yushin, G. *J. Am. Chem. Soc.* **2010**, *132*, 8548.
(5) Wen, C. J.; Huggins, R. A. *J. Solid State Chem.* **1981**, *37*, 271.
(6) Ding, N.; Xu, J.; Yao, Y. X.; Wegner, G.; Fang, X.; Chen, C. H.; Lieberwirth, I. *Solid State Ionics* **2009**, *180*, 222.
(7) Yoshimura, K.; Suzuki, J.; Sekine, K.; Takamura, T. *J. Power Sources* **2007**, *174*, 653.
(8) Heitjans, P.; Schirmer, A.; Indris, S. In *Diffusion in Condensed Matter: Methods, Materials, Models*; Heitjans, P., Kärger, J., Eds.; Springer: Berlin, 2005; Chapter 9, p 369.
(9) Wontcheu, J.; Bensch, W.; Wilkening, M.; Heitjans, P.; Indris, S.; Sideris, P.; Grey, C. P.; Mankovsky, S.; Ebert, H. *J. Am. Chem. Soc.* **2008**, *130*, 288.
(10) Kuhn, A.; Narayanan, S.; Spencer, L.; Goward, G.; Thangadurai, V.; Wilkening, M. *Phys. Rev. B* **2011**, *83*, No. 094302.
(11) Wilkening, M.; Heitjans, P. *Phys. Rev. B* **2008**, *77*, No. 024311.
(12) (a) Nesper, R. *Prog. Solid State Chem.* **1990**, *20*, 1. (b) Okamoto, H. *J. Phase Equilib. Diffus.* **2009**, *30*, 118.
(13) Chevrier, V. L.; Zwanziger, J. W.; Dahn, J. R. *J. Alloys Compd.* **2010**, *496*, 25.
(14) Kubota, Y.; Escano, M. C. S.; Nakanishi, H.; Kasai, H. *J. Appl. Phys.* **2007**, *102*, No. 053704.
(15) Evers, J.; Oehlinger, G.; Sextl, G. *Angew. Chem., Int. Ed. Engl.* **1993**, *32*, 1442.
(16) Axel, H.; Schäfer, H.; Weiss, A. *Z. Naturforsch., B* **1965**, *20*, 1302.
(17) von Schnering, H. G.; Nesper, R.; Curda, J.; Tebbe, K.-F. *Angew. Chem., Int. Ed. Engl.* **1980**, *19*, 1033.
(18) Nesper, R.; von Schnering, H. G.; Curda, J. *Chem. Ber.* **1986**, *119*, 3576.
(19) Bloembergen, N.; Purcell, E.; Pound, R. *Phys. Rev.* **1948**, *73*, 679.
(20) Hendrickson, J.; Bray, P. *J. Magn. Reson.* **1973**, *9*, 341.
(21) Abragam, A. *The Principles of Nuclear Magnetism*; Oxford University Press: Oxford, U.K., 1961.
(22) Sholl, C. A. *J. Phys. C: Solid State Phys.* **1981**, *14*, 447.
(23) Look, D. C.; Lowe, I. J. *J. Chem. Phys.* **1966**, *44*, 2995.
(24) Richards, P. M. *Top. Curr. Phys.* **1979**, *15*, 141.
(25) Mizoguchi, M.; Kume, K.; Shirakawa, H. *Solid State Commun.* **1984**, *50*, 213.
(26) Küchler, W.; Heitjans, P.; Payer, A.; Schöllhorn, R. *Solid State Ionics* **1994**, *70*, 434.
(27) Kuhn, A.; Sreeraj, P.; Pöttgen, R.; Wiemhöfer, H.-D; Wilkening, M.; Heitjans, P. Submitted.
(28) Richards, P. M. *Solid State Commun.* **1978**, *25*, 1019.
(29) Huberman, B. A.; Boyce, J. B. *Solid State Commun.* **1978**, *25*, 759.
(30) Knauth, P. *Solid State Ionics* **2009**, *180*, 911.
(31) Robertson, A. D.; West, A. R.; Ritchie, A. G. *Solid State Ionics* **1997**, *104*, 1.
(32) Thangadurai, V.; Weppner, W. *Ionics* **2006**, *12*, 81.
(33) Heitjans, P.; Koerblein, A.; Ackermann, H.; Dubbers, D.; Fujara, F.; Stoeckmann, H. J. *J. Phys. F: Met. Phys.* **1985**, *15*, 41.